Received: 14 May 2020 | Revised: 11 September 2020 | Accepted: 14 September 2020

DOI: 10.1111/joa.13329

ORIGINAL PAPER

ANATOMICAL SOCIETY Journal of Anatomy WILEY

Microarchitecture of cetacean vertebral trabecular bone among swimming modes and diving behaviors

Danielle N. Ingle | Marianne E. Porter

Department of Biological Sciences, Florida Atlantic University, Boca Raton, FL, USA

Correspondence
Danielle N. Ingle, Department of Biological Sciences, Florida Atlantic University, Boca Raton, FL 33431, USA.
Email: dingle2014@fau.edu

Funding information
This research was supported by funding from Florida Atlantic University and the Marine Technology Society, Florida Education Fund, and Florida Atlantic University to DNI and funds from Florida Atlantic University to MEP. A grant from the United States National Science Foundation (IOS-1941713) to MEP contributed, in part, to this work.

Abstract

Cetaceans (dolphins, whales, and porpoises) are fully aquatic mammals that are supported by water's buoyancy and swim through axial body bending. Swimming is partially mediated by variations in vertebral morphology that creates trade-offs in body flexibility and rigidity between axial regions that either enhance or reduce displacement between adjacent vertebrae. Swimming behavior is linked to foraging ecology, where deep-diving cetaceans glide a greater proportion of the time compared to their shallow-diving counterparts. In this study, we categorized 10 species of cetaceans (Families Delphinidae and Kogiidae) into functional groups determined by swimming patterns (rigid vs. flexible torso) and diving behavior (shallow vs. deep). Here, we quantify vertebral trabecular microarchitecture (a) among functional groups (rigid-torso shallow diver (RS), rigid-torso deep diver (RD), and flexible-torso deep diver (FD)), and (b) among vertebral column regions (posterior thoracic, lumbar, caudal peduncle, and fluke insertion). We microCT scanned vertebral bodies, from which 1-5 volumes of interest were selected to quantify bone volume fraction (BV/TV), specific bone surface (BS/BV), trabecular thickness (TbTh), trabecular number (TbN), trabecular separation (TbSp), and degree of anisotropy (DA). We found that BV/TV was greatest in the rigid-torso shallow-diving functional group, smallest in flexible-torso deep-diving species, and intermediate in the rigid-torso deep-diving group. DA was significantly greater in rigid-torso caudal oscillators than in their flexible-torso counterparts. We found no variation among vertebral regions for any microarchitectural variables. Despite having osteoporotic skeletons, cetacean vertebrae had greater BV/TV, TbTh, and DA than previously documented in terrestrial mammalian bone. Cetacean species are an ideal model to investigate the long-term adaptations, over an animal's lifetime and over evolutionary time, of trabecular bone in non-weight–bearing conditions.

KEYWORDS

bone volume fraction, degree of anisotropy, marine mammal, trabecular thickness, vertebral column region

1 | INTRODUCTION

As a dynamic tissue responsive to load direction and magnitude, trabecular bone structure is closely linked to ecology and habitat use (Biewener et al., 1996; Gray et al., 2007; Ryan & Shaw, 2012, 2015; Wolff, 1892). Extensive research has been conducted on the microarchitecture of bone from terrestrial mammalian vertebrae, which supports the body's axis against gravitational loads (Arlot et al., 2008; Borah et al., 2000; Follet et al., 2011; Mittra et al., 2005; Muller & Ruegsegger, 1997; Teo et al., 2006; Ulrich et al., 1997). However, less in known about the long-term (i.e., multi-year, lifelong, or evolutionary) structural adaptations of vertebral bone in non-weight–bearing conditions (Arfat et al., 2014; Dumont et al., 2013; Ingle & Porter, 2020; in review; Rolvien et al., 2017; Swartz & Middleton, 2008). As mammals that are obligate to aquatic life, where gravitational loads are countered by buoyant forces, cetaceans (dolphins, whales, and porpoises) represent an ideal model to investigate bone structure in non-weight–bearing environments, with potential differences among locomotion modes and behavioral ecology (Berta, 2015; Buchholtz, 2001). Here, we examine microarchitectural variables of vertebral trabecular bone by column region, among cetacean species with varying modes of caudal oscillation and diving behavior.

Mammals secondarily adapted for aquatic life have undergone extensive skeletal modifications throughout evolutionary history, with changes in trabecular bone microstructure predating most gross anatomical shifts (Bajpai, 1998; Gray et al., 2007; Uhen, 2010; Fish, 2016). In contrast to the non-pathological osteoporosis present in modern cetacean skeletons, ancient whale bones were very dense, which aided animals as a bone ballast for foraging in shallow waters (de Buffrenil & Schoevart, 1988; Gray et al., 2007; Taylor, 2000). With the radiation into open-water habitats, cetacean bone became increasingly osteoporotic, determined by evidence of bone resorption within the endosteal lamellae (i.e., Howship lacunae), osteoclastic activity along trabecular struts, and a decreasing compactness of the periosteal cortex throughout life (de Buffrenil & Schoevart, 1988; Gray et al., 2007).

Variation in trabecular microarchitecture has been previously detected in contemporary cetacean vertebrae. Bone volume fraction (BV/TV), or the amount of bone volume per total volume, was about 10% greater in a harbor porpoise (*Phocoena phocoena*) and killer whale (*Orcinus orca*) compared with a sperm whale (*Physeter macrocephalus*), and did not scale with body size (Dumont et al., 2013; Rolvien et al., 2017). Additionally, trabecular mechanical behavior, which is dependent on bone volume and architecture, has been previously shown to vary throughout development and among vertebral morphologies, swimming modes, and diving behaviors in fully aquatic mammalian species (Borah et al., 2000; Ingle and Porter, in review; Kabel et al., 1999; Mittra et al., 2005; Ryan et al., 2010; Ulrich et al., 1997). A study by Ingle & Porter (2020) found that vertebral trabecular mechanical properties varied throughout development in Florida manatees (*Trichechus manatus latirostris*). In *T. manatus latirostris* calves, who experience rapid body growth during the first 2 of years of life, only bone from the posterior region was as strong and tough as in older animals to support undulatory force propagation toward the tail during swimming.

The aim of the present study was to determine vertebral bone 3D microarchitectural variables of cetacean species with different diving behaviors and modes of caudal oscillation. We examined bone volume fraction (BV/TV), specific bone surface (BS/BV), degree of anisotropy (DA), trabecular thickness (TbTh), trabecular number (TbN), and trabecular separation (TbSp) among (a) functional groups (rigid-torso shallow divers (RS), rigid-torso deep divers (RD), and flexible-torso deep divers (FD)), and (b) vertebral column regions (posterior thoracic, lumbar, caudal peduncle, and fluke insertion). We hypothesized that microarchitectural variables among RS, RD, and FD species would vary, and expected highest values in the most active-swimming RS species. We predicted rostrocaudal changes in BV/TV, BS/BV, TbTh, TbN, and TbSp along the length of the vertebral column to support force transmission for fluke-based propulsion since these variables have been shown to correlate with trabecular bone yield strength (Teo et al., 2006).

2 | MATERIALS AND METHODS

We obtained a letter of authorization from the National Marine Fisheries Service (NMFS) for tissue from 10 cetacean species with home ranges extending throughout the southeastern United States (USA) waters (Western Atlantic Ocean). Vertebrae used in this study were obtained from necropsies performed at Mote Marine Laboratory and Aquarium (Sarasota, FL, USA), Harbor Branch Oceanographic Institute Necropsy Laboratory (Fort Pierce, FL, USA), and National Oceanographic and Atmospheric Administration (NOAA) National Marine Fisheries Service (Key Biscayne, FL, and Key Biscayne, LA, USA). Florida Atlantic University's Institutional Animal Care and Use committee approved this tissue protocol (A(T)17-08).

2.1 | Functional groups

To determine ecomorphological differences between closely related cetaceans, we binned 10 species of dolphins and small whales (Order: Cetacea, Parvorder: Odontocete, Families: Delphinidae and Kogiidae) into three functional groups: rigid-torso shallow divers (RS), rigid-torso deep divers (RD), and flexible-torso deep divers (FD; Buchholtz, 2001; Ingle & Porter, in review; Moreno & Carrascal, 1993; Sanderson, 1990). Functional groups were designated based on vertebral morphology, functional interpretations of axial body bending during swimming, and diving behavior (Buchholtz, 2001; Davis et al., 1996; Dolar et al., 2003; Ingle & Porter, in review; Joyce et al., 2017; Klatsky et al., 2007; McAlpine, 2018; Mullin et al., 1994; Mullin & Hansen, 1999; Pulis et al., 2018; Ridgway & Howard, 1979; Scott & Chivers, 2009; Skrovan et al., 1999; Watkins et al., 1987; Wells et al., 2009; Wursig et al., 1994).

2.2 | Rigid-torso shallow divers (RS)

Rigid-torso species were defined by previously documented vertebral centum lengths that were either equal or less than their widths and heights throughout the torso, with a centrum shortening at the fluke insertion. Relatively longer centra were found in the posterior thoracic region and caudal peduncle, indicating areas of greatest translational flexibility (Figure 1a; Buchholtz, 2001; Ingle & Porter, in review; Long et al., 1997; Marchesi et al., 2016). The restricted locomotion in the lumbar vertebral column suggests these cetaceans decrease dorsoventral displacement to increase swimming speeds (Buchholtz, 2001). In the present study, we considered shallow divers as species whose average dive depths do not exceed 50 m, the range beneath which alveolar collapse can occur. Shallow divers may, therefore, actively swim a greater proportion of the time than their deep-diving counterparts (Davis et al., 1996; Klatsky et al., 2007; Scott & Chivers, 2009; Skrovan et al., 1999; Watkins et al., 1987; Williams et al., 2000; Wells et al., 2009). Species (Family Delphinidae) in this functional group include: *Tursiops truncatus* (bottlenose dolphin), *Stenella frontalis* (Atlantic spotted dolphin), *Stenella attenuata* (Pantropical spotted dolphin), *Grampus griseus* (Risso's dolphin), and *Steno bredanensis* (rough-toothed dolphin).

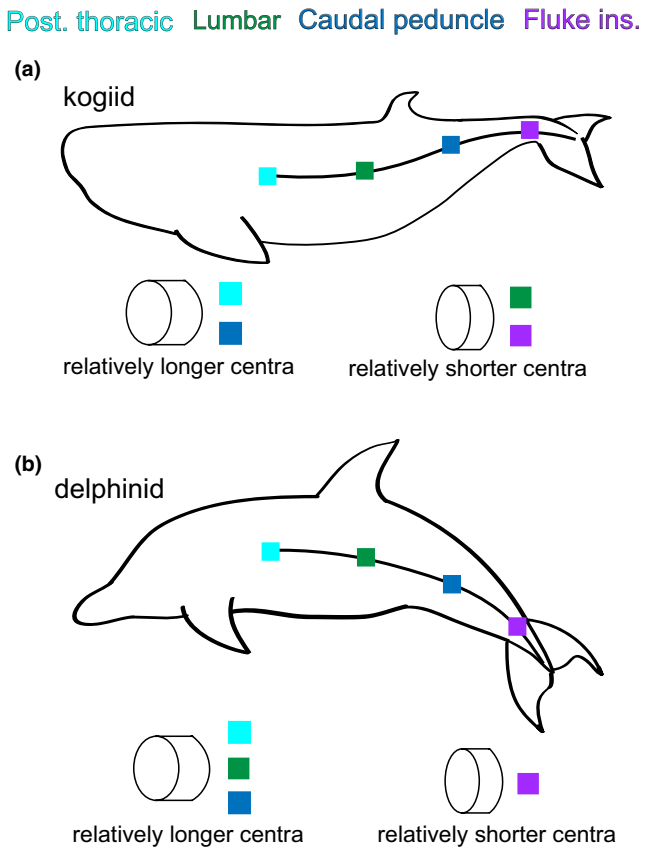

FIGURE 1 Regional sampling and centrum dimensions along the length of the cetacean vertebral column. Vertebrae were sampled from the posterior thoracic (light blue), lumbar (green), caudal peduncle (dark blue) and fluke insertion (purple) regions of the vertebral column; the posterior thoracic through caudal peduncle vertebrae make up the torso. (a) Kogiid centra dimensions were retained from the posterior thoracic to the caudal peduncle region. The posterior thoracic and lumbar regions had the greatest relative centrum lengths, suggesting areas of greatest dorsoventral axial displacement during swimming. (b) Delphinid centra dimensions changed rostrocaudally. Relative centrum lengths were greatest in the posterior thoracic (light blue) and caudal peduncle (dark blue) regions, indicated areas of increased flexibility. Post. Thoracic, Posterior thoracic; Fluke ins., Fluke insertion

2.3 | Rigid-torso deep divers (RD)

Species in this functional group (Family Delphinidae) share similar vertebral dimensions with the shallow-diving delphinids described above (Figure 1a; Buchholtz, 2001; Ingle & Porter, in review). However, these deep divers habitually exceed 100 m, a depth beyond the point in which full alveolar collapse has been noted in bottlenose dolphins (Dolar et al., 2003; Joyce et al., 2017; Pulis et al., 2018; Ridgway & Howard, 1979; Skrovan et al., 1999; Wursig et al., 1994). Once the respiratory system collapses, the animal becomes negatively buoyant and can descend through the water column with a sinking glide (Skrovan et al., 1999). Deep divers may spend a greater percentage of their time gliding compared to animals that mostly forage in shallow waters. RD cetaceans in this study include *Stenella longirostris* (spinner dolphin), *Peponocephala electra* (melon-headed whale), and *Feresa attenuata* (pygmy killer whale).

2.4 | Flexible-torso deep divers (FD)

Previous research described that flexible-torso cetaceans have nearly consistent centrum lengths (which are relatively greater than in delphinids), widths, and heights throughout the torso, and a relative shortening of centra at the fluke insertion (Figure 1b; Buchholtz, 2001; Ingle and Porter, in review). This transition in centrum dimensions suggests the undulatory movement that occurs throughout the torso is interrupted at the fluke, a stiff structure that produces thrust (Buchholtz, 2001). Species in this functional group regularly forage at depths greater than 100 m, experiencing habitual respiratory system collapse, and in this study include *Kogia breviceps* (pygmy sperm whale) and *Kogia sima* (dwarf sperm whale) from Family Kogiidae (McAlpine, 2018; Mullin et al., 1994; Mullin & Hansen, 1999).

2.5 | Vertebral dissection and preparation

We dissected vertebrae from subadult and adult cetaceans, or those at least 3 years old based on species-specific body growth curves. Animals' total lengths ranged between 157 and 278 cm (Table 1; Amano et al., 2014; Amano & Miyazaki, 2004; Bossart et al., 1985; Caldwell & Caldwell, 1989; Ingle & Porter, in review; McAlpine, 2018; Perrin et al., 1976; Siciliano et al., 2007; Stolen et al., 2002).

TABLE 1 Vertebral sampling of kogiid and delphinid species from the present study

					Regional vertebral sampling			
Species	Field ID	Group	TL (cm)	Sex	Post. thor.	Lumbar	Caud. ped.	Fluke ins.
T. truncatus	HBOI1703Tt	RS	201	M	T11	L8	Ca10	Ca19
S. attenuata	GW2015015A	RS	215	F	unknown	L8	Ca9	Ca20
S. frontalis	05ECWR022014	RS	213	M	T12	L8	Ca6	Ca20
S. bredanensis	GW2015009D	RS	232	M	T12	L8	Ca6	no sample
G. griseus	03ECWR02016	RS	278	M	T11	L8	Ca6	Ca19
S. longirostris	MMRSI1612	RD	157	M	T14	L8	Ca7	Ca19
P. electra	HBOI1509Pe	RD	223	M	T11	L8	Ca11	Ca30
F. attenuata	13ECWR091915	RD	211	F	T11	L8	Ca6	Ca19
K. breviceps	GW2015003A	FD	205	M	T11	L8	Ca11	Ca20
K. sima	MARS1701	FD	218	M	T11	L8	Ca2	Ca14

Abbreviations: FD, flexible-torso deep diver; RD, rigid-torso deep diver; RS, rigid-torso shallow diver; TL, total length of each animal.

Our sample included 10 species, and vertebrae were sampled from one animal for each species (Table 1). For all specimens, we sampled vertebrae from the following regions: posterior thoracic, mid-lumbar, anterior caudal (aligned with the anus), and posterior caudal (aligned with the fluke insertion). Once vertebral segments were dissected from the column, they were stored on ice during transport to the laboratory (Florida Atlantic University), where they were wrapped gauze soaked in mammalian Ringer's solution and frozen. Detailed protocols for vertebrae storage and cleaning are previously outline (Ingle & Porter, 2020). Additionally, spinous processes, transverse processes, and chevron bones were removed with a band saw before transportation to Friday Harbor Laboratories (University of Washington).

2.6 | MicroCT scanning

Vertebral bodies were defrosted, packed in plastic canisters with gauze, and scanned in a Bruker SkyScan 1173 (Kontich, Belgium) microcomputed tomography (microCT) machine at Friday Harbor Laboratories. Scans were completed at 25.5-35.1 μm, 60-87 kV, 91-133 μA, and with a 1 mm aluminum filter. Resolutions were selected based on previous settings for mammalian vertebrae with similar sizes (Cotter et al., 2009; Dumont et al., 2013; Eswaran et al., 2007; Marangalou et al., 2014; Saito et al., 2015). Each canister housed 2–6 vertebrae stacked longitudinally, and scan times ranged from 3.5 to 9 hr, after which vertebrae were refrozen. Raw data files from scans were reconstructed using the Bruker NRecon software. Bruker DataViewer software was used to segment vertebrae from one another in multi-vertebrae reconstructed data sets and to orient the vertebral body so that centrum faces were in the superior-inferior axis.

Once all vertebrae were segmented and properly oriented, we used Bruker CTAn software to select a 6 mm substack of images from the center of each vertebral body, from which one to five 6 mm^3 volume of interest (VOI) were selected (Figure 2). Bruker CTAn was used to threshold (i.e., white foreground is bone tissue, black background is non-osseous) substacks of slice data. Specifically, we used the adaptive thresholding algorithm, which has been shown to be more accurate than global thresholding techniques on lower-resolution images (Van Dessel et al., 2013). After thresholding, we then calculated the following 3D microarchitectural variables within each VOI: bone volume fraction (BV/TV; %), or the proportion of trabecular bone voxels relative to the total number of voxels; specific bone surface (BS/BV; %), the ratio of trabecular surface area relative to total trabecular volume; trabecular thickness (TbTh; mm), the mean thickness of trabecular struts; trabecular number (TbN; 1/mm), the number of trabecular struts per mm; trabecular separation (TbSp; mm), the mean width of the spaces between adjacent trabeculae; and degree of anisotropy (DA), the trabecular orientation in 3D space, with larger values denoting a biased arrangement in one direction (Bouxsein et al., 2010; Kivell, 2016).

2.7 | Statistical analyses

We used two-way ANCOVAs to examine differences in BV/TV, BS/BV, TbTh, TbN, TbSp, and DA using functional group (RS, RD, and FD) and region (posterior thoracic, lumbar, caudal peduncle, and fluke insertion) as main effects. We included animal length as a covariate to account for interspecific variability. For each microarchitectural variable, a vertebra is represented as the mean of its VOIs (n = 1-5). *Post-hoc* Tukey tests were conducted to examine differences among significant effects.

Statistical tests were performed using JMP v.5.0.1.a (SAS Institute Inc.), and significance was assigned as $p < .05$. While all statistical tests used the mean microarchitectural variables from each vertebra, our box and whisker plots show data from each VOI (n = 1-5 VOI per vertebra) to show the true range (error bars) of each variable.

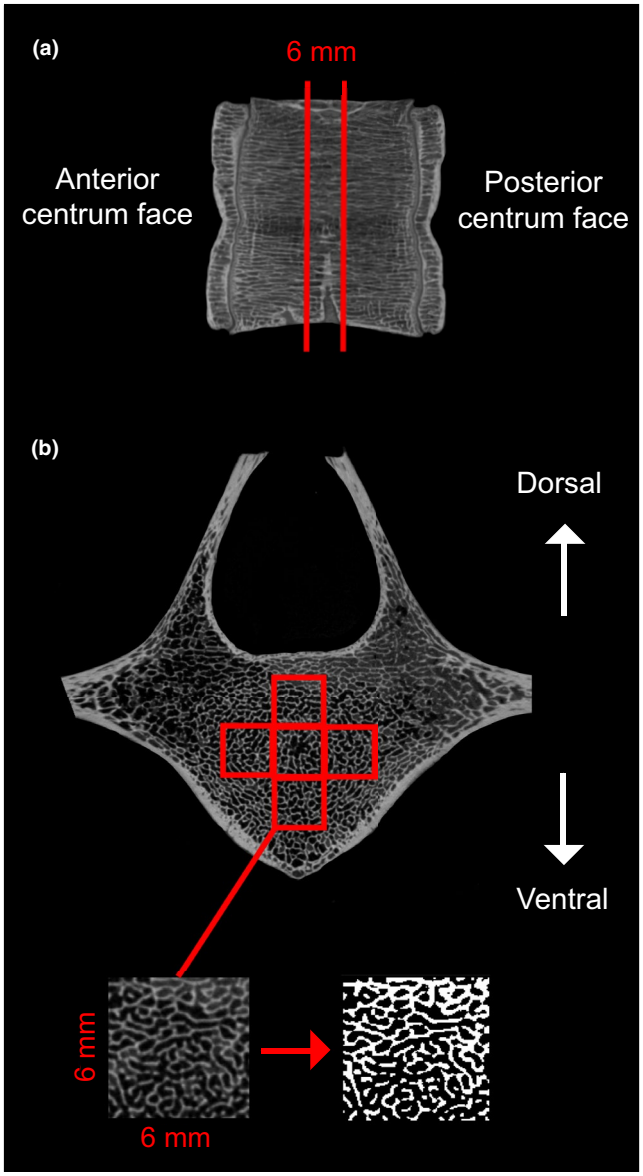

FIGURE 2 Cetacean vertebrae microCT scans. (a) Vertebral body sagittal view. A 6 mm stack was selected from the center of the vertebral body. (b) Frontal view of the stack. Five volumes of interested (VOI; red cubes) were selected from the stack, and each 6 mm cube was thresholded to calculate microarchitectural variables

3 | RESULTS

We used two-way ANCOVAs to evaluate impacts of functional group and region on trabecular architecture: bone volume fraction (BV/TV), specific bone surface (BS/BV), trabecular thickness (TbTh), trabecular number (TbN), trabecular separation (TbSp), and degree of anisotropy (DA); Figure 3; Figure 4). Two-way ANCOVA models were not significant for TbTh ($F_{6,32} = 2.4161$; $p = .059$), BS/BV ($F_{6,32} = 2.3956$; $p = .0503$), TbN ($F_{6,32} = 0.8120$; $p = .5685$), or TbSp ($F_{6,32} = 0.8954$; $p = .5101$; Figure 3; Figure 4).

The two-way ANCOVA examining BV/TV ($F_{6,32} = 8.3043$; $p < .0001$; Figure 4a) was significant, and functional group was a significant main effect ($p < .0001$). Vertebral column region (main effect) and animal length (covariate) were not significant ($p = .1081$ and $p = .1185$; respectively). Tukey *post hoc* tests of functional groups revealed that the greatest trabecular BV/TV and was in RS species (Figure 3a).

The two-way ANCOVA examining DA ($F_{6,32} = 7.6736$; $p < .0001$; Figure 4b) was significant, functional group (main effect) was a significant main effect ($p = .001$), and animal length (covariate) was significant ($p < .0001$). Vertebral column region was not a significant main effect ($p = .3704$). Tukey *post hoc* tests showed the greatest DA was found in the RS and RD functional groups (Figure 3b).

4 | DISCUSSION

This study presents variations in vertebral trabecular bone structure among cetaceans with different swimming modes and diving behaviors. We found that bone volume faction (BV/TV) was greatest in the rigid torso shallow divers (RS) functional group, smallest in flexible-torso deep-diver (FD) species, and intermediate in the rigid torso deep divers (RD) group (Figure 4a). Degree of anisotropy (DA) was significantly greater in rigid-torso (RS and RD) caudal oscillators than in their flexible-torso (FD) counterparts (Figure 4b). No regional variation was detected for any of the microarchitectural variables (Figure 3, 4). Cetacean bone had greater BV/TV, trabecular thickness (TbTh), and DA compared to terrestrial mammals (Table 2). These data suggest that there are long-term adaptations of cetacean bone for non-weight–bearing conditions.

Previous research has described bone volume fraction (BV/TV) and degree of anisotropy (DA) as two of the most biomechanically informative aspects of microarchitecture (Goldstein et al., 1993; Odgaard et al., 1997; van Rietbergen et al., 1998). Indeed, we found the greatest BV/TV and DA in rigid-torso cetaceans, which supports our hypothesis that these species are consistently placing the greatest loads on their vertebral columns (Figures 4, 5). Delphinids, with their stiff, torpedo-shaped body morphologies, are considered some of the fastest odontocetes; Rohr and Fish (2004) found that, on average, delphinids had greater length-specific swimming speeds and fluke-beat frequencies than non-delphinid species (Buchholtz, 2001). By contrast, flexible-torso kogiids, who had the smallest BV/TV and DA, have a swimming modality much more similar to that of baleen whales (Mysticeti), with maximum swimming speeds of only about 2.4 m s^{-1} compared to over 5.7 m s^{-1} documented in wild and captive delphinids (Figures 4, 5; Buchholtz, 2001; Rohr et al., 2002; Scott et al., 2001).

Despite sharing similar skeletal morphologies, rigid-torso shallow-diving species had greater BV/TV compared to their deep-diving delphinid counterparts, a discrepancy which may be driven by the overall proportion of swimming activity. When a diving cetacean surpasses a pivotal threshold of approximately 70 m, their lungs collapse and they utilize negative buoyancy to transition into a gliding descent through the water column (Ridgway & Howard, 1979; Skrovan et al., 1999; Williams et al., 2000). Because they spend

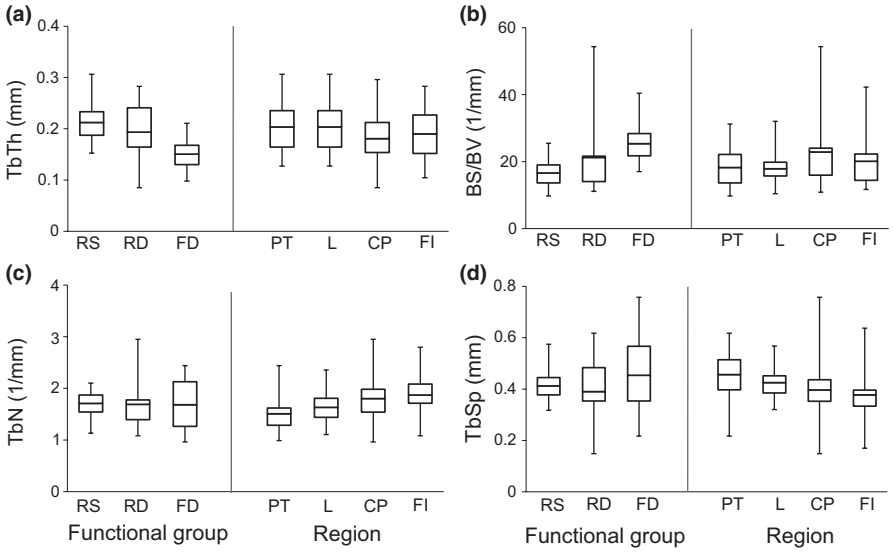

FIGURE 3 We detected no significant differences among functional groups of regions of the vertebral column for the following ANCOVAs (a) trabecular thickness (TbTh; $p = .0590$ (b) specific bone surface (BS/BV; P=0.0503) (c) trabecular number (TbN; $p = .5685$) and (d) trabecular separation (TbSp; $p = .8954$). In each box-and-whisker plot panel, boxes are the 1st and 3rd quartile, line is the mean, and whiskers denote the minimum and maximum values. CP, caudal peduncle; FD, flexibletorso deep-diver; FI, fluke insertion; L, lumbar; PT, posterior thoracic; RD, rigid-torso deep-diver; RS, rigid-torso shallow-diver

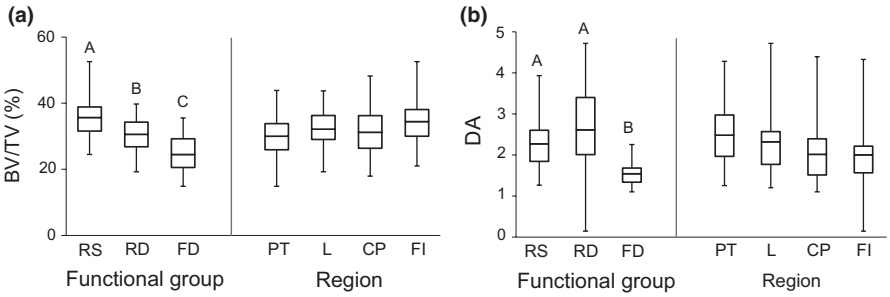

FIGURE 4 Significant ANCOVAs for microarchitectural variables of cetacean vertebral bone among functional groups and regions of the vertebral column. (a) We found that bone volume fraction (BV/TV) was greatest in the rigid-torso shallow-diver (RS) functional group ($p < .0001$). (b) Degree of anisotropy (DA) was significantly greater in the rigid-torso deep-diver (RD) functional group compared to flexible-torso deepdiver (FD) species ($p = .0011$). No regional variations were detected for either BV/TV or DA. In each boxand-whisker plot panel, boxes are the 1st and 3rd quartile, line is the mean, and whiskers denote the minimum and maximum values. CP, caudal peduncle; FI, fluke insertion; L, lumbar; PT, posterior thoracic

TABLE 2 Comparative microarchitectural variables among human, pig, and cetacean vertebral trabecular bone

	Human			Pig	Dolphins and whales
Microarchitectural parameter	Muller and Ruegsegger, 1997	Arlot et al., 2008	Follet et al., 2011	Teo et al., 2006	This study, 2020
BV/TV (%)	8 (0.03)	7.68 (1.19)	7.68 (1.19)	20 (0.07)	30. 26 (5.61)
TbTh (mm)	0.06 (0.02)	0.1 (0.01)	0.14 (0.02)	0.1 (0.01)	0.19 (0.03)
TbN (mm^{-1})	1.30 (0.23)	0.8 (0.2)	0.84 (0.12)	1.70 (0.13)	1.69 (0.01)
TbSp (mm)	0.65 (0.16)	1.3 (0.34)	1.16 (0.19)	0.35 (0.06)	0.42 (0.03)
DA	1.21 (0.06)	1.74 (0.2)	1.68 (0.2)	1.37 (0.07)	2.14 (0.55)

Standard deviations are given between parentheses.

Abbreviations: BV/TV, Bone volume fraction; DA, degree of anisotropy; TbN, trabecular number; TbSp, trabecular separation; TbTh, trabecular thickness.

time gliding, habitual deep divers have increased diving times, which may reduce vertebral column loads and require less trabecular bone to maintain structural integrity of vertebrae against compression compared to shallow divers. However, deep-diving cetacean bone microarchitecture can be influenced by dysbaric osteonecrosis, an end-artery nitrogen embolism pathology, which can be exacerbated when normal diving behavior is altered by anthropogenic disturbances (Jepson et al., 2003; Moore & Early, 2004). Rolvien et al. (2017) found that vertebral bone from sperm whales (*Physeter macrocephalus*), which reach depths of approximately 1,000 m, was

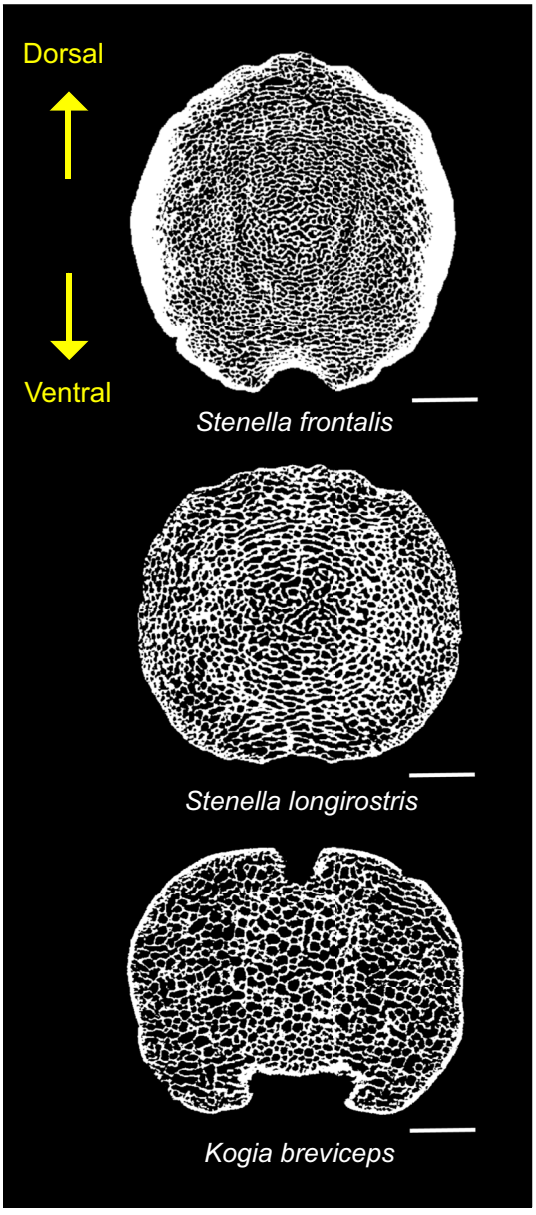

FIGURE 5 Thresholded frontal slices from the center of vertebral bodies located at the fluke insertion of the Atlantic spotted dolphin (Stenella frontalis; rigid-torso shallow-diver (RS)), the spinner dolphin (Stenella longirostris; rigid-torso deep-diver (RD)) and the pygmy sperm whale (Kogia breviceps; flexible-torso deepdiver (FD)). Scale bars = 1 cm

osteocyte-deficient compared to the shallower-diving killer whale (*Orcinus orca*) and harbor porpoise (*Phocoena phocoena*) (Watwood et al., 2006). The present study did not investigate bone histology, and we cannot discount osteonecrosis as a potential factor, especially in the deeper diving pygmy sperm whale and dwarf sperm whale.

Contrary to our hypotheses, we identified no significant variation among functional groups for the other microarchitectural variables, and no regional variation for any variables. Trabecular thickness and specific bone surface (BS/BV) were insignificantly correlated (p = .059 and p = .0503; respectively) for functional groups, but maybe biologically relevant (Figure 3a,b). We hypothesize that the thicker trabeculae in RS species may contribute to the structural needs of bone in active swimming cetaceans. Conversely, greater surface area-to-volume ratios in the flexible-torso deep-diving swimmers suggests less loading of the vertebral column. Further investigation on additional individuals from each functional group will increase sample sizes and may elucidate trends seen in these statistical models. With multiple individuals for every species, future studies can then assess interspecific phylogenetic influences on trabecular structure, which have been previously shown to range from minor to complex (Doube et al., 2011; Houssaye et al., 2014; Ryan & Shaw, 2013).

When compared to previous data on cetacean vertebral bone structure, we found an overall greater bone volume fraction and trabecular thickness, and smaller trabecular number and separation (Rolvien et al., 2017). The inconsistencies between studies may lie within the distribution of volumes of interest throughout the vertebral body for each respective protocol. Rolvien et al. (2017) used punch biopsies to sample throughout cetacean vertebral bodies (endplate-to-endplate) and averaged trabecular microarchitectural variables. We sampled from the center of the vertebral body, where the densest trabecular networks were found in the killer whale, harbor porpoise, and sperm whale (Figure 5; Rolvien et al., 2017). BV/TV found in the center of the vertebral body in killer whales, a delphinid, was 39%, similar to the 36% found in the present study's RS species (Figure 5). In addition, there was virtually no difference in central-vertebrae BV/TV between the deep-diving sperm whale and FD species (25%); these three species are the only extant members of the Superfamily Physeteroidea (Berta, 2015; Rolvien et al., 2017; Watwood et al., 2006). This “bone-within-bone” central densification zone, which is pathological in humans, is described by Rolvien et al., (2017), as an adaptation to withstand the high mechanical demands of caudal oscillatory swimming (Arruda et al., 2016; Fish, 1993; Pabst, 1993; Parry, 1949). The hyperdense center of the vertebral bodies may also serve a ballast function for the body axis of these animals, despite the overall osteoporotic condition of the skeleton (de Buffrenil & Schoevart, 1988; Gray et al., 2007; Taylor, 2000).

We present these data as a contribution to the body of work investigating long-term bone adaptations in non-weight–bearing conditions. Osteoporosis in modern cetaceans is determined by evidence of bone resorption within the endosteal lamellae (i.e., Howship lacunae), osteoclastic activity along trabecular margins, and a decreasing compactness of cortical bone throughout development and into adulthood (de Buffrenil & Schoevart, 1988; Gray et al., 2007). Indeed, Gray et al. (2007) showed that bone from modern cetaceans is hyperporous relative to early transitional counterparts; rib BV/TV showed a decreasing trend throughout evolutionary history with the radiation into pelagic water, ranging from 76% in an ancient semi-aquatic whale (*Gaviacetus sahnii*) to 29% in the extant long-beaked common dolphin (*Delphinus capensis*). Bone mass reflects habitual loads on an animal's skeletal

system, and BV/TV, TbTh, and DA were surprisingly greater than in human and pig vertebrae, despite the weight-bearing lifestyle of these terrestrial mammals (Table 2; Arlot et al., 2008; de Buffrenil & Schoevart, 1988; Follet et al., 2011; Frost, 1987; Gray et al., 2007; Muller & Ruegsegger, 1997; Teo et al., 2006). These data may reflect the relatively high locomotor demands placed on the cetacean vertebral column by axial muscles, which are extremely robust and commensurate with body size (Parry, 1949). As highly derived swimmers, dolphin caudal oscillation can produce maximum mass-specific thrust powers of 35.3 W kg^{-1}, compared to powers of only 0.5 W kg^{-1} during human breast stroke swimming and 6.5 W kg^{-1} during human running (Miyashita, 1974; Pabst, 1990; Fish, 1993; Cavagna et al., 2005).

In addition to mechanosensory responses, other factors may affect variations in trabecular bone structure. Many of the delphinid and kogiid species in the present study feed primarily on fatty fish rich in vitamin D, which promotes bone formation, and calcidiol (vitamin D metabolite) in the blood of free-ranging bottlenose dolphins was over four times the amount detected in human blood (Bender, 2003; Berta, 2015; Gimmel et al., 2016). Therefore, diet, in combination with other non-locomotor aspects of biology, may influence the vertebral inner-architecture of these wild cetaceans, whose natural history is largely unknown.

This study quantified the microarchitectural variables of vertebral trabecular bone from several cetacean species. We found that the rigid-torso shallow-diving functional group had the greatest bone volume fraction and degree of anisotropy while flexible-torso deep-diving species had the smallest values; we hypothesized that differences may be driven by varying modes of caudal oscillation, swimming speed, and diving behavior. Despite having osteoporotic skeletons, we found that cetacean vertebral bone had greater microarchitectural variables compared to previously investigated terrestrial mammals, and we hypothesize that these data reflect a structural adaptation to support loads imparted on the vertebral column through caudal oscillatory swimming. As mammals that became obligate swimmers over 30 MYA, we present cetaceans as an ideal longitudinal *in situ* model for the long-term adaptations of bone in a non-weight–bearing environment.

ACKNOWLEDGMENTS

We thank A. Summers from the Karl F. Liem Imaging Facility (University of Washington Friday Harbor Laboratories; San Juan Islands, WA) and the FAU High School Owls Imaging Lab (Florida Atlantic University; Boca Raton, FL) for providing microCT scanner (Bruker SkyScan 1173) access and laboratory space for data collection, and M. Gerringer and A. Bahadur for help with training on the equipment and Bruker software. Thank you to NSF (DEB-1701665), who funded microCT scanning at the Karl F. Liem Imaging Lab. We gratefully acknowledge the Marine Technology Society, Florida Education Fund, and Florida Atlantic University for funding. We also thank Mote Marine Laboratory and Aquarium (Sarasota, FL), NOAA National Marine Fisheries Service (Key Biscayne, FL, and Key Biscayne, LA, USA), Harbor Branch Oceanographic Institute (Fort Pierce, FL), and especially W. Marks for help with vertebrae collection, transport, and storage.

DATA AVAILABILITY STATEMENT

The dataset generated and analyzed in the current study are available in the Open Science Framework repository. https://doi.org/10.17605/OSF.IO/4RZ8X

ORCID

Danielle N. Ingle https://orcid.org/0000-0002-1759-0604
Marianne E. Porter https://orcid.org/0000-0002-3622-7114

REFERENCES

Amano, M. & Miyazaki, N. (2004) Composition of a school of risso's dolphins, grampus griseus. *Marine Mammal Science*, 20(1), 152–160.
Amano, M., Yamada, T.K., Kuramochi, T., Hayano, A., Kazumi, A. & Sakai, T., et al. (2014) Life history and group composition of melon-headed whales based on mass strandings in Japan. *Marine Mammal Science*, 30(2), 480–493.
Arfat, Y., Xiao, W.-Z., Iftikhar, S., Zhao, F., Li, D.-J., Sun, Y.-L., et al. (2014) Physiological effects of microgravity on bone cells. *Calcif Tissue Int*, 94(6), 569–579.
Arlot, M.E., Burt-Pichat, B., Roux, J.P., Vashishth, D., Bouxsein, M.L. & Delmas, P.D. et al. (2008) Microarchitecture influences microdamage accumulation in human vertebral trabecular bone. *Journal of Bone and Mineral Research*, 23(10), 1613–1618.
Arruda, M., Coelho, M.C.A., Moraes, A.B., de Paula Paranhos-Neto, F., Madeira, M., Farias, M.L.F. et al. (2016) Bone mineral density and microarchitecture in patients with autosomal dominant osteopetrosis: A report of two cases. *Journal of Bone and Mineral Research*, 31(3), 657–662.
Bajpai, S. & Gingerich, P.D. (1998) A new Eocene archaeocete (Mammalia, Cetacea) from India and the time of origin of whales. *Proceedings of the National Academy of Sciences of the United States of America*, 95(26), 15464–15468.
Bender, D.A. (2003) *Vitamin D. Nutritional biochemistry of the vitamins*. Cambridge: Cambridge University Press.
Berta, A. (Ed.). (2015) *Whales, dolphins, and porpoises: A natural history and species guide*. Chicago: University of Chicago Press.
Biewener, A.A., Fazzalari, N.L., Konieczynski, D.D. & Baudinette, R.V. (1996) Adaptive changes in trabecular architecture in relation to functional strain patterns and disuse. *Bone*, 19(1), 1–8.
Borah, B., Dufresne, T.E., Cockman, M.D., Gross, G.J., Sod, E.W., Myers, W.R. et al. (2000) Evaluation of changes in trabecular bone architecture and mechanical properties of minipig vertebrae by three-dimensional magnetic resonance microimaging and finite element modeling. *Journal of Bone and Mineral Research*, 15(9), 1786–1797.
Bossart, G.D., Odell, D.K. & Altman, N.H. (1985) Cardiomyopathy in stranded pygmy and dwarf sperm whales. *Journal of the American Veterinary Medical Association*, 187(11), 1137–1140.
Bouxsein, M.L., Boyd, S.K., Christiansen, B.A., Guldberg, R.E., Jepsen, K.J. & Müller, R. (2010) Guidelines for assessment of bone microstructure in rodents using micro–computed tomography. *Journal of Bone and Mineral Research*, 25(7), 1468–1486.
Buchholtz, E.A. (2001) Vertebral osteology and swimming style in living and fossil whales (Order: Cetacea). *Journal of Zoology*, 253(2), 175–190.
de Buffrenil, V. & Schoevaert, D. (1988) On how the periosteal bone of the delphinid humerus becomes cancellous: Ontogeny of a histological specialization. *Journal of Morphology*, 198(2), 149–164.
Caldwell, D.K. & Caldwell, M.C. (1989) Pygmy sperm whale Kogia breviceps (de Blainville, 1838): Dwarf sperm whale Kogia simus Owen, 1866. *Handbook of Marine Mammals*, 4, 235–260.

Cavagna, G.A., Heglund, N.C. & Willems, P.A. (2005) Effect of an increase in gravity on the power output and the rebound of the body in human running. *Journal of Experimental Biology*, 208(12), 2333–2346.

Cotter, M.M., Simpson, S.W., Latimer, B.M. & Hernandez, C.J. (2009) Trabecular microarchitecture of hominoid thoracic vertebrae. *Anatomical Record*, 292(8), 1098–1106.

Davis, R.W., Worthy, G.A., Würsig, B., Lynn, S.K. & Townsend, F.I. (1996) Diving behavior and at-sea movements of an Atlantic spotted dolphin in the Gulf of Mexico. *Marine Mammal Science*, 12(4), 569–581.

Dolar, M.L.L., Walker, W.A., Kooyman, G.L. & Perrin, W.F. (2003) Comparative feeding ecology of spinner dolphins (*Stenella longirostris*) and Fraser's dolphins (*Lagenodelphis hosei*) in the Sulu Sea. *Marine Mammal Science*, 19(1), 1–19.

Doube, M., Kłosowski, M.M., Wiktorowicz-Conroy, A.M., Hutchinson, J.R. & Shefelbine, S.J. (2011) Trabecular bone scales allometrically in mammals and birds. *Proceedings of the Royal Society B: Biological Sciences*, 278(1721), 3067–3073.

Dumont, M., Laurin, M., Jacques, F., Pellé, E., Dabin, W. & de Buffrénil, V. (2013) Inner architecture of vertebral centra in terrestrial and aquatic mammals: A two-dimensional comparative study. *Journal of Morphology*, 274(5), 570–584.

Eswaran, S.K., Allen, M.R., Burr, D.B. & Keaveny, T.M. (2007) A computational assessment of the independent contribution of changes in canine trabecular bone volume fraction and microarchitecture to increased bone strength with suppression of bone turnover. *J Biomech*, 40(15), 3424–3431.

Fish, F.E. (1993) Power output and propulsive efficiency of swimming bottlenose dolphins (Tursiops truncatus). *Journal of Experimental Biology*, 185(1), 179–193.

Fish, F.E. (2016) Secondary evolution of aquatic propulsion in higher vertebrates: validation and prospect. *Integrative and Comparative Biology*, 56(6), 1285–1297.

Follet, H., Viguet-Carrin, S., Burt-Pichat, B., Dépalle, B., Bala, Y., Gineyts, E., et al. (2011) Effects of preexisting microdamage, collagen crosslinks, degree of mineralization, age, and architecture on compressive mechanical properties of elderly human vertebral trabecular bone. *Journal of Orthopaedic Research*, 29(4), 481–488.

Frost, H.M. (1987) Bone "mass" and the "mechanostat": A proposal. *The Anatomical Record*, 219(1), 1–9.

Gimmel, A.E.R., Baumgartner, K. & Liesegang, A. (2016) Vitamin blood concentration and vitamin supplementation in bottlenose dolphins (Tursiops truncatus) in European facilities. *BMC Veterinary Research*, 12(1), 180.

Goldstein, S.A., Goulet, R. & McCubbrey, D. (1993) Measurement and significance of three-dimensional architecture to the mechanical integrity of trabecular bone. *Calcified Tissue International*, 53(S1), S127–S133.

Gray, N.M., Kainec, K., Madar, S., Tomko, L. & Wolfe, S. (2007) Sink or swim? Bone density as a mechanism for buoyancy control in early cetaceans. *The Anatomical Record: Advances in Integrative Anatomy and Evolutionary Biology*, 290(6), 638–653.

Houssaye, A., Tafforeau, P. & Herrel, A. (2014) Amniote vertebral microanatomy–what are the major trends? *Biological Journal of the Linnean Society*, 112(4), 735–746.

Ingle, D.N. & Porter, M.E. (in review). Cetacean trabecular bone mechanical properties vary among functional groups and vertebral column regions. *Proceedings of the Royal Society B*.

Ingle, D.N. & Porter, M.E. (2020) Developmental changes in bone mechanics from Florida manatees (Trichechus manatus latirostris), obligate swimming mammals. *Journal of Experimental Biology*, 223(6), 1–11.

Jepson, P.D., Arbelo, M., Deaville, R., Patterson, I.A.P., Castro, P., Baker, J.R., et al. (2003) Gas-bubble lesions in stranded cetaceans. *Nature*, 425(6958), 575–576.

Joyce, T.W., Durban, J.W., Claridge, D.E., Dunn, C.A., Fearnbach, H., Parsons, K.M., et al. (2017) Physiological, morphological, and ecological tradeoffs influence vertical habitat use of deep-diving toothed-whales in the Bahamas. *PLoS One*, 12(10), e0185113.

Kabel, J., Odgaard, A., van Rietbergen, B. & Huiskes, R. (1999) Connectivity and the elastic properties of cancellous bone. *Bone*, 24(2), 115–120.

Kivell, T.L. (2016) A review of trabecular bone functional adaptation: what have we learned from trabecular analyses in extant hominoids and what can we apply to fossils? *Journal of Anatomy*, 228(4), 569–594.

Klatsky, L.J., Wells, R.S. & Sweeney, J.C. (2007) Offshore bottlenose dolphins (*Tursiops truncatus*): movement and dive behavior near the Bermuda Pedestal. *Journal of Mammalian*, 88(1), 59–66.

Long, J.H., Pabst, D.A., Shepherd, W.R. & Mclellan, W.A. (1997) Locomotor design of dolphin vertebral columns: Bending mechanics and morphology of Delphinus delphis. *Journal of Experimental Biology*, 200(1), 65–81.

Marangalou, J.H., Eckstein, F., Kuhn, V., Ito, K., Cataldi, M., Taddei, F. & Van Rietbergen, B. (2014) Locally measured microstructural parameters are better associated with vertebral strength than whole body density. *Osteoporosis International*, 25(4), 1285–1296.

Marchesi, M.C., Pimper, L.E., Mora, M.S. & Goodall, R.N.P. (2016) The vertebral column of the hourglass dolphin (Lagenorhynchus cruciger Quoy and Gaimard, 1824): With notes on its functional properties in relation to its habitat. *Aquatic Mammals*, 42(3), 306–316.

McAlpine, D.F. (2018). Pygmy and dwarf sperm whales: Kogia breviceps and K. sima. In B. Wursig, J.G.M. Thewissen, & K. Kovacs (Eds.), *Encyclopedia of marine mammals* (3rd ed., pp. 786–788). London & San Diego: Academic Press.

Mittra, E., Rubin, C. & Qin, Y.X. (2005) Interrelationship of trabecular mechanical and microstructural properties in sheep trabecular bone. *Journal of Biomechanics*, 38(6), 1229–1237.

Miyashita, M. (1974) Method of calculating mechanical power in swimming the breast stroke. *Research Quarterly. American Alliance for Health, Physical Education and Recreation*, 45(2), 128–137.

Moore, M.J. & Early, G.A. (2004) Cumulative sperm whale bone damage and the bends. *Science*, 306(5705), 2215.

Moreno, E. & Carrascal, L.M. (1993) Leg morphology and feeding postures in four *Parus* species: An experimental ecomorphological approach. *Ecology*, 74(7), 2037–2044.

Muller, R. & Ruegsegger, P. (1997) Micro-tomographic imaging for the nondestructive evaluation of trabecular bone architecture. *Studies in Health Technology and Informatics*, 40, 61–79.

Mullin, K.D. & Hansen, L.J. (1999) Marine mammals in the northern Gulf of Mexico. In: Kumph, H., Steidinger, K. and Sherman, K. (Eds.) *The Gulf of Mexico large marine ecosystem: Assessment, sustainability and management*. New York: Blackwell Science, (pp. 736).

Mullin, K.D., Hoggard, W., Roden, C.L., Lohoefener, R.R., Rogers, C.M. & Taggart, B. (1994) Cetaceans on the upper continental slope in the north-central Gulf of Mexico. *Fish Bull*, 92(4), 773–786.

Odgaard, A., Kabel, J., van Rietbergen, B., Dalstra, M. & Huiskes, R. (1997) Fabric and elastic principle directions of cancellous bone are closely related. *Journal of Biomechanics*, 30(5), 487–495.

Pabst, D.A. (1990) Axial muscles and connective tissue of the bottlenose dolphin. In: Leatherwood, S. and Reeves, R.R. (Eds.) *The bottlenose Dolphin*. San Diego and London: Academic Press, pp. 51–67.

Pabst, D.A. (1993) Intramuscular morphology and tendon geometry of the epaxial swimming muscles of dolphins. *Journal of Zoology*, 230(1), 159–176.

Parry, D.A. (1949) The structure of whale blubber, and a discussion of its thermal properties. *Journal of Cell Science*, 3(9), 13–25.

Perrin, W.F., Coe, J.M. & Zweifel, J.R. (1976) Growth and reproduction of the spotted porpoise, *Stenella attenuata*, in the offshore eastern tropical Pacific. *Fish Bull*, 74(2), 229–269.

Pulis, E.E., Wells, R.S., Schorr, G.S., Douglas, D.C., Samuelson, M.M. & Solangi, M. (2018) Movements and dive patterns of pygmy killer whales (*Feresa attenuata*) released in the Gulf of Mexico following rehabilitation. *Aquatic Mammals*, 44(5), 555–567.

Ridgway, S.H. & Howard, R. (1979) Dolphin lung collapse and intramuscular circulation during free diving: Evidence from nitrogen washout. *Science*, 206(4423), 1182–1183.

van Rietbergen, B., Odgaard, A., Kabel, J. & Huiskes, R. (1998) Relationships between bone morphology and bone elastic properties can be accurately quantified using high-resolution computer reconstructions. *Journal of Orthopaedic Research*,, 16(1), 23–28.

Rohr, J.J. & Fish, F.E. (2004) Strouhal numbers and optimization of swimming of odontocete cetaceans. *J Exp Biol*, 207(10), 1633–1642.

Rohr, J.J., Fish, F.E. & Gilpatrick, J.W. Jr (2002) Maximum swim speeds of captive and free-ranging delphinids: Critical analysis of extraordinary performance. *Marine Mammal Science*, 18(1), 1–19.

Rolvien, T., Hahn, M., Siebert, U., Püschel, K., Wilke, H.J., Busse, B., et al. (2017) Vertebral bone microarchitecture and osteocyte characteristics of three toothed whale species with varying diving behaviour. *Sci Rep*, 7(1), 1–10.

Ryan, W.F., Lynch, P.B. & O'Doherty, J.V. (2010) Survey of cull sow bone and joint integrity in the Moorepark Research Farm herd. *Veterinary Record*, 166(9), 268–271.

Ryan, T.M. & Shaw, C.N. (2012) Unique suites of trabecular bone features characterize locomotor behavior in human and non-human anthropoid primates. *PLoS One*, 7(7), e41037.

Ryan, T.M. & Shaw, C.N. (2013) Trabecular bone microstructure scales allometrically in the primate humerus and femur. *Proceedings of the Royal Society B: Biological Sciences*, 280(1758), 20130172.

Ryan, W.F. & Shaw, C.N. (2015) Gracility of the modern Homo sapiens skeleton is the result of decreased mechanical loading. *Proceedings of the National Academy of Sciences of the United States*, 112(2), 372–377.

Saito, M., Kida, Y., Nishizawa, T., Arakawa, S., Okabe, H., Seki, A. & Marumo, K. (2015) Effects of 18-month treatment with bazedoxifene on enzymatic immature and mature cross-links and non-enzymatic advanced glycation end products, mineralization, and trabecular microarchitecture of vertebra in ovariectomized monkeys. *Bone*, 81, 573–580.

Sanderson, S.L. (1990) Versatility and specialization in labrid fishes: Ecomorphological implications. *Oecologia*, 84(2), 272–279.

Scott, M.D. & Chivers, S.J. (2009) Movements and diving behavior of pelagic spotted dolphins. *Marine Mammal Science*, 25(1), 137–160.

Scott, M.D., Hohn, A.A., Westgate, A.J., Nicolas, J.R., Whitaker, B.R., & Campbell, W.B. (2001) A note on the release and tracking of a rehabilitated pygmy sperm whale (*Kogia breviceps*). *Journal of Cetacean Research and Management*, 3(1), 87–94.

Siciliano, S., Ramos, R.M.A., di Beneditto, A.P.M., Santos, M.C.O., Fragoso, A.B., Brito, J.L. et al. (2007) Age and growth of some delphinids in south-eastern Brazil. *Journal of the Marine Biological Association of the United Kingdom*, 87(1), 293–303.

Skrovan, R.C., Williams, T.M., Berry, P.S., Moore, P.W. & Davis, R.W. (1999) The diving physiology of bottlenose dolphins (Tursiops truncatus). II. Biomechanics and changes in buoyancy at depth. *Journal of Experimental Biology*, 202(20), 2749–2761.

Stolen, M.K., Odell, D.K. & Barros, N.B. (2002) Growth of bottlenose dolphins (*Tursiops trucatus*) from the Indian River Lagoon system, Florida, U.S.A. *Marine Mammal Science*, 18(2), 348–357.

Swartz, S.M. & Middleton, K.M. (2008) Biomechanics of the bat limb skeleton: scaling, material properties and mechanics. *Cells Tissues Organs*, 187(1), 59–84.

Taylor, M.A. (2000) Functional significance of bone ballast in the evolution of buoyancy control strategies by aquatic tetrapods. *Historical Biology*, 14(1–2), 15–31.

Teo, J.C.M., Si-Hoe, K.M., Keh, J.E.L. & Teoh, S.H. (2006) Relationship between CT intensity, micro-architecture and mechanical properties of porcine vertebral cancellous bone. *Clin Biomech Elsevier Ltd*, 21(3), 235–244.

Uhen, M.D. (2010) The origin (s) of whales. *Annual Review of Earth and Planetary Sciences*, 38, 189–219.

Ulrich, D., Hildebrand, T., van Rietbergen, B., Muller, R. & Ruegsegger, P. (1997) The quality of trabecular bone evaluated with micro-computed tomography, FEA, and mechanical testing. *Studies in Health Technology and Informatics*, 40, 97–112.

Van Dessel, J., Huang, Y., Depypere, M., Rubira-Bullen, I., Maes, F. & Jacobs, R. (2013) A comparative evaluation of cone beam CT and micro-CT on trabecular bone structures in the human mandible. *Dentomaxillofacial Radiology*, 42(8), 20130145.

Watkins, W.A., Tyack, P., Moore, K.E. & Notarbartolo-di-Sciara, G. (1987) *Steno bredanensis* in the Mediterranean Sea. *Marine Mammal Science*, 3(1), 78–82.

Watwood, S.L., Miller, P.J., Johnson, M., Madsen, P.T. & Tyack, P.L. (2006) Deep-diving foraging behaviour of sperm whales (*Physeter macrocephalus*). *Journal of Animal Ecology*, 75(3), 814–825.

Wells, R., Manire, C., Byrd, L., Smith, D., Gannon, J., Fauquier, D. & Mullin, K. (2009) Movements and dive patterns of a rehabilitated Risso's dolphin, *Grampus griseus*, in the Gulf of Mexico and Atlantic Ocean. Publications, Agencies and Staff of the US Department of Commerce, p. 26.

Williams, T.M., Davis, R.W., Fuiman, L.A., Francis, J., Le, B.J., Horning, M., et al. (2000) Sink or swim: Strategies for cost-efficient diving by marine mammals. *Science*, 288(5463), 133–136.

Wolff, J. (1892) *Das Gesetz der Transformation der Knochen*. Berlin: Verlag von August Hirschwald.

Wursig, B., Wells, R.S. & Norris, K.S. (1994) Food and feeding. In: K.S. Norris, B. Wursig, R.S. Wells and M. Wursig (Eds.) *The Hawaiian spinner dolphin*. California: University of California Press, pp. 216–232.

How to cite this article: Danielle NI, Marianne EP. Microarchitecture of cetacean vertebral trabecular bone among swimming modes and diving behaviors. *J. Anat.* 2020;00:1–10. https://doi.org/10.1111/joa.13329